

Quantum phase transitions and quantum chaos in generalized Dicke and Jahn-Teller polaron model and finite-size effects

Eva Majerníková^{1,*} and Serge Shpyrko^{2,†}

¹*Institute of Physics, Slovak Academy of Sciences,
Dúbravská cesta 9, SK-84 511 Bratislava, Slovak Republic*

²*Institute for Nuclear Research, Ukrainian
Academy of Sciences, pr. Nauki 47, Kiev, Ukraine*

Abstract

The Dicke model extended to two bosons of different frequencies or equivalent generalized Jahn-Teller lattice model are shown to exhibit a spontaneous quantum phase transition between the polaron-modified "quasi-normal" and squeezed "radiation" phase with the transition point dependent on the frequencies. In a finite lattice a mixed domain of coexistence of the quasi-normal and modified radiation phase is created within the quasi-normal phase domain. There occurs a field-directed oscillation-assisted tunneling (hopping). The field is driven by simultaneous squeezing and polaron-dressing of the collective boson level mode due to the additional boson mode. In a finite lattice in the radiation domain there occurs a sequence of local tunnelings (oscillations) between two minima of a local potential weakly coupled to two assisting oscillations. The "radiation" phase reveals itself as an almost ideal instanton-anti-instanton gas phase. The correlations among the energy levels mediated by the additional mode in the mixed domain considerably reduce the level repulsions. As a consequence, the Wigner level spacing probability distribution of the two-boson Dicke model is non-universally reduced from the Wigner to the semi-Poisson and asymptotically to the Poisson distribution of level spacings. The correlations cause a suppression of the coherence of the radiation phase as finite-size effect. Possible applications of the present theory are suggested.

PACS numbers: 63.22.-m, 05.45.Mt, 73.43.Nq, 31.30.-i

*Electronic address: eva.majernikova@savba.sk

†e-mail: serge.shp(at)yahoo.com

I. INTRODUCTION

The class of nonintegrable pseudospin-boson lattice models with one [1, 2, 3, 4, 5, 6, 7] or two boson modes of different local symmetry [8, 9, 10, 11] gained a long-term interest in condensed matter physics and quantum optics. They exhibit a rich variety of interesting statistical properties, e.g., quantum and thermodynamic phase transitions and quantum chaos in energy spectra revealed in spectral statistics.

In the Dicke model [5] the quantum spontaneous phase transition was found from the effectively unexcited "normal" phase to the "super-radiant" phase, a macroscopically excited and highly collective state [6, 7]. A collective spontaneous emission of coherent radiation is due to the cooperative interaction of a large number of two-level atoms all excited to the upper state (Dicke maser). The transition from quasi-integrability to quantum chaos is given by a localization-delocalization transition as a precursor of the phase transition [7] in which the ground state wave function bifurcates into a macroscopic superposition for any finite number of atoms. Theoretical and experimental research of the superradiance or superfluorescence of photons and spontaneous emission of phonons in various variants of the Dicke-like collective system ([12, 13, 14, 15, 16]) still remains in a focus of interest ([17, 18, 19, 20]).

If a dephasing mechanism suppresses the strict coherence, processes based on collective spontaneous emission will reveal incoherent nature depending on the strength of the dephasing and some peculiar effects result: Luminescence spectra of rare gas solids, alkali halides (iodides) and some crystals based on fullerenes comprise two contributions at low temperatures: a broadband ascribed to selftrapped excitons and, at higher energies, narrow-line (-band) optical transitions, fluorescence and stimulated emission with sharply structured absorption and emission transitions and a line-narrowing with inhomogeneous broadening due to free excitons. Spontaneous emission reflected in fluorescence or luminescence spectra was first observed as a free-exciton resonance luminescence coexisting with the broadband luminescence of the selftrapped excitons excited by electrons or synchrotron radiation in rare gas solids and alkali halides (iodides) [21] and later by other authors [22, 23]. Transition from superfluorescence to amplified spontaneous emission with lost coherence was studied on super-oxide ion in potassium chloride in the intermediate regime as a function of temperature [23]. Similar effects were observed also in structures based on Jahn-Teller (JT) active

molecules, e.g., fullerenes C_{60} [24]. Laser-induced fluorescence line narrowing experiment of C_{60} -hydroquinone crystals demonstrates inhomogeneous broadening of the zero-phonon lines. Similar observation has been done on Dicke superfluorescence in KCl [25] and the broadening was ascribed to unspecified internal strains. The peculiar high-energy narrow band luminescence in the exciton and Jahn-Teller bearing structures has been proposed to be caused by the emission from the localized "exotic" excited states within the phonon-selftrapped spectrum by Wagner et al. [26, 27] (these states correspond to the tunneling states proposed by Slonczewski [28]).

Direct observation of the dynamic Jahn-Teller effect in C_{60} [29] brought an evidence of important role of the ionic motion in the electron-phonon interaction. The quantum fluctuations led to formation of the tunneling states between two energy wells of the distorted phase (selftrapped electrons) which pertain to the undistorted geometry and recover free electron motion found theoretically [26, 27, 30]. This picture corresponds to the concept of coexistence of selftrapped states and tunneling to localized (exotic) states at higher energies.

Physical interest in JT models is motivated by importance of some spatially anisotropic complex structures (fullerenes, manganites, perovskites, etc) which exhibit JT structural phase transition. The transition is due to large local distortions related to the electron selftrapping. The JT model is a prototype model for electron coupling to two degenerate intramolecular vibrons of the same frequency (see (6) below) removing the degeneracy of electron levels (α -term) and phonon-mediated tunneling between the split levels (β -term). Respective vibron spectrum is complex with level crossings and avoidings and needs exact diagonalization of matrices of confined level manifolds and proper statistical methods of evaluation. In crystals exhibiting high spatial anisotropy the rotation symmetry of JT molecules ($\alpha = \beta$, $\Omega_1 = \Omega_2$, Ω_i being frequencies of the vibron modes) is generally broken. Therefore, it is reasonable to investigate the JT model assuming different coupling strengths for the onsite intralevel (α) and interlevel (β) electron-phonon couplings and different vibron frequencies. Such a model can also be considered as a generalization of the exciton-phonon or dimer-phonon model, assuming the electron tunneling to be phonon-assisted. It implies a competition of the selftrapping distortion mechanism (localization) and a quantum tunneling (delocalization) one.

We will show that the lattice JT Hamiltonian of molecules with degenerate electron levels coupled with two non-equivalent boson (vibron) modes is formally equivalent to the Dicke

Hamiltonian generalized by adding a boson mode coupled with the level spacing. We shall investigate their excited spectra and related statistical properties vs those of the one-boson Dicke model. An impact of the additional boson mode which removes the double degeneracy of the JT electron levels close to the quantum phase transition from normal to super-radiant phase reveals as a finite-size effect of level correlations mediated by the additional boson. We will study analytically an interplay of quantum fluctuations and symmetry breaking and numerically related characteristic signatures of a quantum chaos - the level spacing probability distributions, spectral entropies and spectral densities. We will demonstrate the localization-delocalization transition of the wave functions within the available lattice at the point of the phase transition between the quasi-normal and radiation phase. As for applications, we shall propose a zero temperature mechanism of the coherence dephasing and the broadening of the spectra, including the broadening of the zero-phonon lines. Further, we propose a similar impact on the quantum localization-delocalization phase transition from the Mott insulator to the superfluid state of ultracold atoms in optical lattices.

Let us first shortly summarize the basic attributes of the Dicke model in order to motivate our use of the collective Holstein-Primakoff bosonization method for the two-boson JT model. The exciton-boson (photon, phonon) model of a lattice chain of N atoms is represented by the Hamiltonian

$$H = \sum_k \Omega_k a_k^\dagger a_k + \omega_0 \sum_{n=1}^N \sigma_z^{(n)} + \lambda \frac{1}{\sqrt{N}} \sum_{n=1}^N \sum_k (a_k^\dagger \exp(ikn) + a_k \exp(-ikn)) \left(\sigma_+^{(n)} + \sigma_-^{(n)} \right), \quad (1)$$

where $\sigma_i^{(n)}$ are spin variables; n is a chain site, N is the size of the chain, $k = \pm\pi l/N$, $l = 0, 1, \dots, N$ is the wave vector of the phonon wave, Ω_k is the photon (phonon) frequency of the k -th mode, ω_0 is the level spacing and λ is the level-phonon interaction strength. Phonon creation and annihilation operators a_k^\dagger , a_k satisfy conventional commutation rules $[a_k, a_k^\dagger] = 1$. The coefficient $1/\sqrt{N}$ arises from the dipole coupling strength [7]. This factor allows also for the correct account of the transition to the thermodynamic limit $N \rightarrow \infty$. The Dicke model is obtained from the model (1) when the boson is supposed homogeneous (of long wave length) within a finite set of lattice sites, $|k| \ll \pi$. Then, the collective spin variables $J_z = \sum_n \sigma_z^{(n)}$, $J_+ + J_- = \frac{1}{\sqrt{N}} \sum_n \left(\sigma_+^{(n)} + \sigma_-^{(n)} \right)$ over all atoms in the chain can be introduced [5] and the Dicke Hamiltonian yields

$$H = \Omega a^\dagger a + \omega_0 J_z + \lambda \frac{1}{\sqrt{N}} (a^\dagger + a)(J_+ + J_-). \quad (2)$$

The collective (N-dimensional) spin variables J_z , J_+ , J_- satisfy the same commutation relations as the individual spins:

$$[J_z, J_{\pm}] = \pm J_{\pm}; \quad [J_+, J_-] = 2J_z \quad (3)$$

with $J_x = \frac{1}{2}(J_+ + J_-)$, $J_y = -\frac{i}{2}(J_+ - J_-)$. It is handy to represent the realization of the spin operators of higher dimensions by the Dicke states. Each Dicke state is labeled as $|j, m\rangle$ with the discrete index m ranging (at fixed j) from $-j, -j+1, \dots$ to j . The spin operators in the Dicke space are defined as follows:

$$J_z|j, m\rangle = m|j, m\rangle; \quad J_{\pm}|j, m\rangle = \sqrt{j(j+1) - m(m \pm 1)}|j, m \pm 1\rangle; \quad J^2|j, m\rangle = j(j+1)|j, m\rangle. \quad (4)$$

The subspaces of the Dicke states labeled by j are independent and, hence, one can consider them separately keeping j fixed. For the chain containing N atoms possible values of j range as $0, 1, \dots, N/2$ for N even and $1/2, 3/2, \dots, N/2$ for N odd; for given j the operators J_i are matrices with dimensions $2j+1$ (representations of the $SU(2)$ group). The parity operator

$$\Pi = \exp\{i\pi(a^\dagger a + J_z + j)\}, \quad (5)$$

commutes with Hamiltonian (2), i.e. the number of excitation quanta $\langle a^\dagger a \rangle + J_z + j$ is conserved within a phase. Namely, the space of states is separated onto two subspaces with the number of excitation quanta which is either even or odd [6, 7]. Then the split subspaces can be considered separately. This conservation is broken at the quantum phase transition.

Two-level pseudospin-vibron (photon) JT model Hamiltonian investigated in [32, 33, 34] has the form of the 2×2 matrix which in the pseudospin notation is written as

$$H = \Omega(a_1^\dagger a_1 + a_2^\dagger a_2 + 1)I + \alpha(a_1^\dagger + a_1)\sigma_z - \beta(a_2^\dagger + a_2)\sigma_x \quad (6)$$

Hamiltonian (6) describes the electron-boson interaction in a two-level JT molecule with two boson modes a_i of equal frequencies Ω (I in the first term is the unity matrix). In (6), the α -coupled mode lifts the double degeneracy of the local JT level and β -coupled mode mediates the electron tunneling between the split levels [31]. Different electron-boson coupling strengths α and β present a generalization with reference to the conventional (rotational symmetric) JT model where $\alpha = \beta$ [34].

In a similar way as for the exciton model (1) a natural generalization of the two-level pseudospin-vibron (photon) JT Hamiltonian can be done by extending the dimensionality of

the (pseudo)spin space. Namely, the generalized model considered within the present work is characterized by the following Hamiltonian:

$$H = \Omega_1 \left(\frac{1}{2} + a_1^\dagger a_1 \right) I + \Omega_2 \left(\frac{1}{2} + a_2^\dagger a_2 \right) I + \frac{\alpha}{\sqrt{2j}} (a_1^\dagger + a_1) \cdot 2J_z + \frac{\beta}{\sqrt{2j}} (a_2^\dagger + a_2) (J_+ + J_-). \quad (7)$$

The operators J are defined in representation of the $SU(2)$ group (3) in a $2j + 1$ -dimensional space spanned by Dicke vectors $|j, m\rangle$ as described above (Eq.(4)). We assume a general case of the rotation symmetry breaking with different boson frequencies Ω_1 and Ω_2 .

In the molecular JT model the bosons represent the intramolecular vibrons. The rotational symmetry is broken by taking different frequencies and interaction parameters $\alpha \neq \beta$. The generalization acquires a twofold interpretation: (i) The JT lattice model, j lattice sites represent a finite number of identical JT molecules, i.e. two-level molecules coupled to two intramolecular vibrons (of the same intramolecular structure). Then the electron collective coordinate can be introduced representing a collective spin of N two-level molecules (ensemble of qubits) coupled with two local vibron modes identical for each on-site molecule. (ii) The excited on-site molecule with two intra-molecular vibrons can be considered by taking a set of many excited (j) levels of the molecule. (7) can be then interpreted as usual many-level system (a single atom with a spin $\geq 1/2$) coupled to two boson modes.

The above concept of JT model can be applied, e. g., for the formulation of the JT polaron model in nanostructures where due to their finite size the quantum effects are rather detectable for observation.

Additionally the photonic JT model [10, 11] with collective boson modes homogeneous within the chain of atoms is within the scope of (7) as well.

In the Dicke model, two bosons represent optical fields of the wave length larger than the size of the lattice and so they enable to introduce the collective variables for the electron levels. Mathematically, both the generalized Dicke and JT models are then equivalent and represented by equation (7).

Thus an impact of the coupling of the level spacing with the additional boson a_1 compared to the conventional one-boson Dicke model (2) is to be studied.

Likewise in the exciton model there exists the same operator of parity $\Pi = \exp\{i\pi(a_2^\dagger a_2 + J_z + j)\}$, which commutes with Hamiltonian (7). For the JT molecule with only two electron

levels ($j = 1/2$) and equal boson frequencies this fact reflects itself in the conserved parity $p = \pm 1$ [31, 32] as an additional good quantum number. For parities $+1$ and -1 the spectra of that model are identical. As we shall see, for the present generalization this is the case of even number of molecules, that is for the main Dicke numbers $j = 1/2, 3/2, \dots$.

Finally, a diagonal term of the form ΔJ_z can be added to the (7) where the parameter Δ accounts for the intrinsic level separation. This term accounts for a magnetic field [11]. In the JT model, this term is known to affect the shape of the adiabatic potential: it lifts the conical intersection of upper and lower adiabatic surfaces.

Number and relative values of the pseudospin-boson couplings involved are of essential importance for specification of statistical properties of the pseudospin-boson models: while the excited spectra of various pseudospin-one-boson models were found to exhibit Wigner chaos when approaching the semiclassical limit [1, 2, 3, 4, 6, 7], the excited spectra of the molecular JT model ($\Omega_1 = \Omega_2$) exhibit nonuniversal chaotic behaviour between the Poisson and semi-Poisson limit [33, 34, 35]. The antisymmetric against reflection level splitting mode a_1 of the JT model increases by one the number of local degrees of freedom when compared to the exciton model. Simultaneously, this phonon (photon) mode mediates additional level correlations and quantum fluctuations and thus it weakens the level repulsions. The interaction effects are modified by the frequency difference and are expected to imply an impact on the statistical properties of the lattice models such as quantum phase transition to the super-radiant phase and proper statistical characteristics of the quantum chaos.

In Section II we investigate numerically and analytically the ground state and related phase transition of the extended Dicke model or, equivalently, of the lattice JT model (7) with two bosons of different frequencies. For analytical calculations we use the Holstein-Primakoff bosonization Ansatz for the pseudospin variables. We analyze the macroscopic phases for three involved oscillators related to the competing correlations (self-trapping and squeezing) due to the additional mode. In Section III we present analytical investigations of the interplay of quantum fluctuations and the symmetry breaking as a useful insight into the scenario leading to the macroscopic phase transition in the system of three oscillators. For a finite lattice, within the quasi-normal domain a medium quantum domain is shown to be created in which both the "normal" and "radiation" phase coexist. In Section IV we present numerical results on wave functions and statistical properties of excited states, namely level spacing probability distributions for various number of lattice sites, values of frequencies and

coupling parameters and compare them with those of the one-boson Dicke model. Further, the distribution of occupation of excited states over the lattice sites is illustrated by the state entropies as functions of quantum numbers of even states. The spectral densities as functions of energy are calculated as illustration of the effect of the interaction with the boson modes on the spectral density on the Dicke spectral space. The wave functions and the statistical characteristics reflect the medium quantum domain as being mixed from the localized and delocalized contributions of the normal and radiation phase, respectively.

For presentation of some numerical results we use the resonance case $\Omega_1 = \Omega_2$ except for the cases where the difference of the frequencies makes qualitative changes. Throughout all the paper we shall use the term "radiation" phase for our model with suppressed coherence instead of the term "super-radiant" standardly used for the strictly coherent one-boson Dicke model.

II. GROUND STATE AND PHASE TRANSITION

Use of the method of collective pseudospin variables for two-level electron-boson JT and Dicke lattice models is appropriate under the conditions presented in Introduction. The collective coordinates enable solving these nonintegrable models efficiently, though approximately. In what follows, we apply them for the investigation of a lattice of JT molecules or the two-boson Dicke model.

Hamiltonian of the system can be written as a generalized version of (1) ($k = 0$) as follows

$$H = \Omega_1 \left(\frac{1}{2} + a_1^\dagger a_1 \right) I + \Omega_2 \left(\frac{1}{2} + a_2^\dagger a_2 \right) I + \sum_{i=1}^N \frac{1}{\sqrt{2j}} \left[\alpha (a_1^\dagger + a_1) 2s_z^{(i)} + \beta (a_2^\dagger + a_2) (s_+^{(i)} + s_-^{(i)}) \right], \quad (8)$$

where j assumes values in different subspaces $j = 0, 1, 2, \dots, N/2$ for N even and $j = 1/2, 3/2, \dots, N/2$ for N odd. In what follows we will always take into consideration only the subspace with largest $j = N/2$ for each number of atoms in a chain. The frequencies of both modes are Ω_1, Ω_2 and corresponding coupling constants are α, β . Introducing the collective coordinates J_i defined by (3) into equation (8) in the same fashion as for (1) we arrive at Hamiltonian (7) representing either the generalized Dicke or JT lattice model. For $j = 1/2$, the local (molecular) JT model (with broken rotational symmetry if $\alpha \neq \beta$, $\Omega_1 \neq \Omega_2$) is recovered. For completeness, the standard Dicke-like model is the one-boson

version of Hamiltonian (7) without assistance of the bosons 1.

For analytical treatment it is convenient to bosonize the spin variables in the two-boson-spin system (7) using the Holstein-Primakoff Ansatz [37]

$$J_z = b^\dagger b - j, \quad J_+ = b^\dagger \sqrt{2j - b^\dagger b}, \quad J_- = \sqrt{2j - b^\dagger b} b \quad (9)$$

for the collective pseudospin operators. Here, b are fictitious boson operators, $[b, b^\dagger] = 1$. This representation of the spin algebra preserves exactly the commutation relations (3) and makes it possible to convert the system to two or three coupled quantum oscillators as will be shown below.

Linear terms in the Hamiltonian (7) can be excluded by the use of the coherent state representation with boson displacements chosen variationally. Let us displace the operators involved as follows

$$a_1^\dagger = c_1^\dagger + \sqrt{\alpha_1}, \quad a_2^\dagger = c_2^\dagger + \sqrt{\alpha_2}, \quad b^\dagger = d^\dagger - \sqrt{\delta}. \quad (10)$$

Applying the Holstein-Primakoff Ansatz (9), setting (10) into (7) and expanding the square root expressions in (9) to first order terms in $d^\dagger d$ yields the form

$$\begin{aligned} H = & \Omega_1 \left(\frac{1}{2} + c_1^\dagger c_1 \right) + \Omega_2 \left(\frac{1}{2} + c_2^\dagger c_2 \right) + \Omega_1 \alpha_1 + \Omega_2 \alpha_2 + \Omega_1 \sqrt{\alpha_1} (c_1^\dagger + c_1) + \Omega_2 \sqrt{\alpha_2} (c_2^\dagger + c_2) \\ & + \frac{2\alpha}{\sqrt{2j}} \left[(c_1^\dagger + c_1) d^\dagger d + 2\sqrt{\alpha_1} d^\dagger d - \sqrt{\delta} (c_1^\dagger + c_1) (d^\dagger + d) - 2\sqrt{\alpha_1} \delta (d^\dagger + d) + (\delta - j) (c_1^\dagger + c_1) \right. \\ & + \left. 2\sqrt{\alpha_1} (\delta - j) \right] + \frac{\beta}{\sqrt{2j}} (c_2^\dagger + c_2 + 2\sqrt{\alpha_2}) \cdot k \left\{ -2\sqrt{\delta} + (1 - \delta/k^2) (d^\dagger + d) + \frac{\sqrt{\delta}}{k^2} d^\dagger d \right. \\ & \left. + \frac{1}{2k^2} \left[-(d^{\dagger 2} d + d^\dagger d^2) + \sqrt{\delta} ((d^\dagger + d)^2 - 1) \right] \right\}, \quad k \equiv \sqrt{2j - \delta}. \quad (11) \end{aligned}$$

From the condition of elimination of the terms linear in boson operators from (11) three identities for the parameters α_i and δ follow:

$$\begin{aligned} \Omega_1 \sqrt{\alpha_1} &= -\frac{2\alpha}{\sqrt{2j}} (\delta - j), \\ \Omega_2 \sqrt{\alpha_2} &= \frac{\beta \sqrt{\delta}}{\sqrt{2j}} \frac{4j - 2\delta + 1/2}{\sqrt{2j - \delta}}, \\ \sqrt{\delta} (\delta - j) &\left(4\Omega_2 \alpha^2 - 2\Omega_1 \beta^2 \frac{4j - 2\delta + 1/2}{2j - \delta} \right) = 0. \end{aligned} \quad (12)$$

It we consider a finite lattice (j finite), this set of equations implies three solutions provided $\Omega_2 \alpha^2 \neq \Omega_1 \beta^2(1 + 1/8j)$ as follows:

$$1. \sqrt{\alpha_1} = \frac{\alpha}{\Omega_1} \sqrt{2j}, \quad \alpha_2 = 0, \quad \delta = 0, \quad (13)$$

$$2. \alpha_1 = 0, \quad \sqrt{\alpha_2} = \frac{\beta}{\Omega_2} \sqrt{2j} \left(1 + \frac{1}{4j}\right), \quad \delta = j, \quad (14)$$

$$3. \sqrt{\alpha_1} = -\frac{\alpha}{\Omega_1} \sqrt{2j}(1 - 2\bar{\mu}), \quad \sqrt{\alpha_2} = \frac{\alpha^2}{\Omega_1} \frac{2\sqrt{2j}}{\beta} \sqrt{\bar{\mu}(1 - \bar{\mu})}, \quad \delta = 2j(1 - \bar{\mu}), \quad (15)$$

where in the last set $\bar{\mu} = \frac{\beta^2 \Omega_1}{8j(\alpha^2 \Omega_2 - \beta^2 \Omega_1)} \equiv \frac{\bar{\beta}^2}{8j(\alpha^2 - \bar{\beta}^2)} < 1$, and $\alpha > \bar{\beta} \equiv \sqrt{\Omega_1/\Omega_2} \beta$.

As will be seen in the next subsections, first two solutions in the thermodynamic limit $j \rightarrow \infty$ account for the common “normal” and “super-radiant” phases of a system, the transition between them at $\alpha\sqrt{\Omega_2} = \beta\sqrt{\Omega_1}$ describing the quantum phase transition (QPT) similar to what was reported for the Dicke models of superradiance [6, 7, 9, 18]. The third solution in the thermodynamic limit becomes trivially degenerated and valid only on the line of the said QPT. Nontrivial consequences for this solution arise for finite j only: From Eqs. (13) and (14) a transition to the rotational symmetry of the two-dimensional vibron oscillator is evident at $\alpha_2 = \alpha_1$ at the critical point $\alpha = \beta\sqrt{\frac{\Omega_1}{\Omega_2}}(1 + 1/4j)$. In the limit of large $j \rightarrow \infty$ this is the point of the phase transition described below. This limit of higher symmetry exhibits qualitatively different properties when compared with the case $\alpha \neq \beta\sqrt{\Omega_1/\Omega_2}(1 + 1/4j)$ and j finite as we shall see in Section IV. Let us note, that the factors like $\sim 1/j$ are the origin of specific quantum effects such as the squeezing of the frequency $\omega_2 = \frac{4\beta^2}{\Omega_2} \cosh(4r)$, $\cosh 4r = 1 + 1/4j$, of the oscillator (polaron) 2 (subsection B). The effect of squeezing gets implications for the level spacing probability distributions especially in the case 3 when all three oscillators are coupled (Subsection C).

A. Case 1: Polaron self-trapping in the normal phase.

The solution (13) represents the normal phase with average zero number of macroscopically excited electron level bosons $\delta = 0$. Hamiltonian (11) related to this solution reads

$$H_1 = \Omega_1 \left(\frac{1}{2} + c_1^\dagger c_1\right) + \Omega_2 \left(\frac{1}{2} + c_2^\dagger c_2\right) + \frac{4\alpha^2}{\Omega_1} (d^\dagger d - j/2) + \beta(c_2^\dagger + c_2)(d^\dagger + d) + \frac{2\alpha}{\sqrt{2j}} (c_1^\dagger + c_1)d^\dagger d - \frac{\beta}{4j} (c_2^\dagger + c_2)(d^{\dagger 2}d + d^\dagger d^2). \quad (16)$$

Here, the level oscillator acquires the frequency of a polaron- dressed oscillator $\omega_1 = 4\alpha^2/\Omega_1$ which results from the self-trapping by the additional mode in contrast with respective factor of the Dicke model ω_0 . Explicit interaction of the oscillator modes with the level bosons contribute only to excited states $\propto 1/\sqrt{j}$ in (16). Thus, in the limit $j \rightarrow \infty$ Hamiltonian (16) recovers the normal phase Hamiltonian of polaron level oscillators. For large j only linear terms persist (first line in (16)) and it can be easily diagonalized by a rotation in the plane of coupled operators c_2 and d [7] to yield the form

$$H_{1d} = \Omega_1 c_1^\dagger c_1 + \epsilon_{1,+} C_2^\dagger C_2 + \epsilon_{1,-} C_3^\dagger C_3 - \frac{2\alpha^2}{\Omega_1} j \quad (17)$$

with new effective oscillators C_2, C_3 . The excitation energies of the system $\epsilon_{1,\pm}$ are

$$\epsilon_{1,\pm}^2 = \frac{1}{2} \left(\Omega_2^2 + \omega_1^2 \pm \left[(\Omega_2^2 - \omega_1^2)^2 + 64\alpha^2\beta^2 \frac{\Omega_2}{\Omega_1} \right]^{1/2} \right). \quad (18)$$

From (18), the solution for ϵ_1 exists provided $\omega_1 > 4\beta^2/\Omega_2 \equiv \omega_2$, or if $\alpha\sqrt{\Omega_2} > \beta\sqrt{\Omega_1}$. This phase is identified as the normal phase of the Dicke-like model without macroscopic excitations, Fig. 1. The effect of different initial frequencies $\Omega_1 \neq \Omega_2$ is just the shift of the phase transition point supporting the phase with the smaller of Ω_i .

From (16), critical Hamiltonian $H_1^{crit} = H_1(\beta_c = \alpha\sqrt{\Omega_2/\Omega_1})$ at the point of the phase transition yields

$$H_1^{crit} = \sqrt{\Omega_2^2 + \left(\frac{4\alpha^2}{\Omega_1}\right)^2} \left(C_2^\dagger C_2 + 1/2 \right) + \Omega_1 (c_1^\dagger c_1 + 1/2) - \frac{2\alpha^2 j}{\Omega_1}. \quad (19)$$

The coupled undisplaced oscillators a_2 and b form an effective single oscillator of the frequency $\sqrt{\Omega_2^2 + (4\alpha^2/\Omega_1)^2}$. The mixing results from the coupling due to the assisting oscillator a_2 between the levels split by the oscillator a_1 . The additional coherent oscillator c_1 remains decoupled.

B. Case 2: Squeezing in the radiation phase.

The second solution (14) identified further with the superradiant phase, can be treated on the same footing. For this solution the level bosons (9) are displaced by $\delta = j$ that is

they acquire a macroscopic number of excited quanta. Respective Hamiltonian (11) yields

$$\begin{aligned}
H_2 = & \Omega_1 \left(\frac{1}{2} + c_1^\dagger c_1 \right) + \Omega_2 \left(\frac{1}{2} + c_2^\dagger c_2 \right) + \frac{2\beta^2}{\Omega_2} \left(1 + \frac{1}{4j} \right) \left(d^\dagger d - j - \frac{1}{4} \right) - \sqrt{2}\alpha(c_1^\dagger + c_1)(d^\dagger + d) \\
& + \frac{\beta^2}{\Omega_2} \left(1 + \frac{1}{4j} \right) (d^\dagger + d)^2 + \frac{2\alpha}{\sqrt{2j}}(c_1^\dagger + c_1)d^\dagger d + \frac{\beta}{\sqrt{2j}}(c_2^\dagger + c_2)d^\dagger d + \frac{\beta}{2\sqrt{2j}}(c_2^\dagger + c_2) \\
& \times \left[(d^\dagger + d)^2 - \frac{1}{\sqrt{j}}(d^{\dagger 2}d + d^\dagger d^2) \right] - \frac{\beta^2}{\Omega_2\sqrt{j}} \left(1 + \frac{1}{4j} \right) (d^{\dagger 2}d + d^\dagger d^2) . \tag{20}
\end{aligned}$$

Linear part of (20) relevant in approaching the thermodynamic limit $j \rightarrow \infty$ represents the level polaron coupled with the oscillator 1. Quantum fluctuations squeeze its frequency by the squeezing parameter $\cosh 4r = (1 + 1/4j)$. Transformation of this part of (20) by the unitary operator of squeezing $S = \exp[r(d^{\dagger 2} - d^2)]$ using the identities

$$\begin{aligned}
\tilde{d}^\dagger \tilde{d} & \equiv S d^\dagger d S^{-1} = d^\dagger d \cosh 4r + \sinh^2 2r + (d^2 + d^{\dagger 2}) \frac{1}{2} \sinh 4r, \\
(\tilde{d}^\dagger + \tilde{d}) & \equiv S(d^\dagger + d)S^{-1} = (d^\dagger + d)e^{-2r} \tag{21}
\end{aligned}$$

yields the squeezed polaronic oscillator with renormalized frequency $\omega_2 = 4\beta^2/\Omega_2 \cosh(4r)$ and interaction $\kappa = \sqrt{2}\alpha e^{2r}$,

$$\tilde{H}_2 = \Omega_1 \left(\frac{1}{2} + c_1^\dagger c_1 \right) + \Omega_2 \left(\frac{1}{2} + c_2^\dagger c_2 \right) + \omega_2 \tilde{d}^\dagger \tilde{d} - \kappa(c_1^\dagger + c_1)(\tilde{d}^\dagger + \tilde{d}) - \frac{2\beta^2}{\Omega_2} j - \omega_2 \sinh^2 2r . \tag{22}$$

Diagonalization of (22) implies three independent oscillators C_1, C_3 and c_2 , last one remaining free,

$$H_{2d} = \epsilon_{2,+} C_3^\dagger C_3 + \epsilon_{2,-} C_1^\dagger C_1 + \Omega_2 c_2^\dagger c_2 - \frac{2\beta^2}{\Omega_2} j , \tag{23}$$

where

$$\epsilon_{2,\pm}^2 = \frac{1}{2} \left(\Omega_1^2 + \omega_2^2 \pm \left[(\Omega_1^2 - \omega_2^2)^2 + 64\alpha^2\beta^2 e^{4r} \frac{\Omega_1}{\Omega_2} \right]^{1/2} \right) . \tag{24}$$

Energy of the squeezed ground state is $H_{2G} = -2\beta^2/\Omega_2 \cdot j - \omega_2 \sinh^2 2r$. From (24), one obtains the condition for stability of the radiation phase

$$\frac{\beta^2}{\Omega_2} > \frac{\alpha^2}{\Omega_1} e^{4r} . \tag{25}$$

Let us remind that for $j \rightarrow \infty$ the squeezing parameter $r \rightarrow 0$ ($\sinh 4r \sim 1/\sqrt{2j}$).

Close to the phase transition point $\beta_c = \alpha\sqrt{\Omega_2/\Omega_1}$ where $\epsilon_1^{(-)} = 0$, we can find the energy from the side of the normal phase $\alpha \rightarrow \beta_{c-}$

$$\epsilon^{(-)} \rightarrow \frac{8\alpha^{3/2}\Omega_2^{3/4}}{\sqrt{2}(\Omega_1^2\Omega_2^2 + 16\alpha^4)^{1/2}} \left(\alpha\sqrt{\Omega_2} - \beta\sqrt{\Omega_1} \right)^{1/2} . \tag{26}$$

From the side of the radiation phase, at $\beta_{c+} \leftarrow \alpha_+$, the energy reads

$$\epsilon^{(+)} \rightarrow \frac{8 \beta^{3/2} \Omega_1^{3/4} e^{2r}}{\sqrt{2} \left(\Omega_1^2 \Omega_2^2 + 16 \beta^4 \right)^{1/2}} \left(\beta \sqrt{\Omega_1} - \alpha \sqrt{\Omega_2} \right)^{1/2}. \quad (27)$$

In the limit $j \rightarrow \infty$ the squeezing parameter r vanishes, and the energy dependence becomes symmetric with simultaneous interchange $\alpha \leftrightarrow \beta$, $\Omega_1 \leftrightarrow \Omega_2$. Note that in the resonance case $\Omega_1 = \Omega_2$ the cusps in (26), (27) are symmetric around the critical point $\alpha = \beta$ (Fig. 1). However, for finite j this symmetry is broken because of the factor $\exp(2r)$ in the numerator of (27): the radiation phase (27) is suppressed by the squeezing when compared to the normal phase. The non-symmetry of the branches below and above the critical point is also evident from numerical results for the excitation energy from the exact Hamiltonian (7) presented in Fig. 1. Let us note, that the critical exponent $1/2$ near the critical point in (26) and (27) is characteristic for the mean field second order phase transition. The branches (26) and (27) represent a generalized version of the branches by Emary and Brandes [7]: The analogy becomes obvious if we set $\lambda_c = \frac{1}{2} \sqrt{\omega \omega_0} \equiv \sqrt{\frac{\Omega_1}{\Omega_2}} \beta_c$, with $\omega \equiv \Omega_1 = \Omega_2$, $\omega_0 \equiv 4\alpha^2/\Omega_1$.

In the limit $j \rightarrow \infty$, similar critical behavior as (19) can be found for the energy of the phase 2, $H_2^{crit} = H_2(\sqrt{\frac{\Omega_1}{\Omega_2}} \beta_c = \alpha)$. From (23), one obtains

$$H_2^{crit} = \sqrt{\Omega_1^2 + \left(\frac{4\beta^2}{\Omega_2} \right)^2} (C_1^\dagger C_1 + 1/2) + \Omega_2 (c_2^\dagger c_2 + 1/2) - \frac{2\alpha^2}{\Omega_1} j, \quad (28)$$

where now the displaced oscillator c_2 remains decoupled and the undisplaced oscillator c_1 mediates a mixing with the split level polaronic oscillators of the frequency $\omega_2 = 4\beta^2/\Omega_2$.

The analysis of both phases shows that within linear approximation the oscillator c_1 in the radiation phase plays qualitatively the same role as it does the oscillator c_2 with simultaneous interchange of the polaron frequencies $\omega_1 \leftrightarrow \omega_2$ (coupling constants $\alpha \leftrightarrow \beta \sqrt{\frac{\Omega_1}{\Omega_2}}$). Hence, in linear approximation two oscillators mix to two-dimensional effective oscillator while the remaining one is decoupled. For the resonant case $\Omega_1 = \Omega_2$ and $\alpha = \beta$ ($\omega_1 = \omega_2$) a spontaneous transition occurs (in the plane of vibron coordinates (Q_1, Q_2)) to the rotation symmetric two-dimensional oscillator of a qualitatively different behavior which is out of the scope of this paper. This case implies an abrupt change of the statistical characteristics of the quantum excited levels (section IV) related to the higher symmetry of the problem [33].

C. Case 3. Intermediate domain of mixed quasi-normal and "radiation" phase

The solution (15), valid for finite j , implies for Hamiltonian (11) following form

$$\begin{aligned}
H_3 = & \Omega_1 \left(\frac{1}{2} + c_1^\dagger c_1 \right) + \Omega_2 \left(\frac{1}{2} + c_2^\dagger c_2 \right) + \frac{4\alpha^2 \bar{\mu}}{\Omega_1} d^\dagger d - \\
& 2\alpha \sqrt{1 - \bar{\mu}} (c_1^\dagger + c_1) (d^\dagger + d) + \beta \frac{2\bar{\mu} - 1}{\sqrt{\bar{\mu}}} (c_2^\dagger + c_2) (d^\dagger + d) + \\
& \frac{2\alpha^2}{\Omega_1} (1 - \bar{\mu}) (d^\dagger + d)^2 + \frac{2\alpha}{\sqrt{2j}} (c_1^\dagger + c_1) d^\dagger d + \frac{\beta}{\sqrt{2j}} \frac{\sqrt{1 - \bar{\mu}}}{\sqrt{\bar{\mu}}} (c_2^\dagger + c_2) d^\dagger d \\
& + \frac{\beta}{2\sqrt{2j}} \frac{\sqrt{1 - \bar{\mu}}}{\sqrt{\bar{\mu}}} (c_2^\dagger + c_2) (d^\dagger + d)^2 \\
& - \frac{2\alpha^2}{\Omega_1 \sqrt{2j}} (1 - \bar{\mu})^{1/2} (d^{\dagger 2} d + d^\dagger d^2) - \frac{\beta}{4j \sqrt{\bar{\mu}}} (c_2^\dagger + c_2) (d^{\dagger 2} d + d^\dagger d^2) - \\
& \frac{2\alpha^2}{\Omega_1} j (1 - 2\bar{\mu})^2 + \frac{8\alpha^4 \Omega_2 j}{\beta^2 \Omega_1^2} \bar{\mu} (1 - \bar{\mu}) - \frac{2\alpha^2 (1 - \bar{\mu})}{\Omega_1} - \frac{16\alpha^2 j \bar{\mu} (1 - \bar{\mu})}{\Omega_1}, \tag{29}
\end{aligned}$$

where $\bar{\mu} = \frac{\beta^2 \Omega_1}{8j(\alpha^2 \Omega_2 - \beta^2 \Omega_1)} < 1$, $\alpha > \beta \sqrt{\frac{\Omega_1}{\Omega_2}}$.

From (29) one obtains for the quasi-classical oscillators $\langle c_1^\dagger + c_1 \rangle \equiv q_1 \sqrt{2\Omega_1}$, $\langle c_2^\dagger + c_2 \rangle \equiv q_2 \sqrt{2\Omega_2}$ and for the level polaron $\langle d^\dagger + d \rangle = Q \sqrt{8\alpha^2 \bar{\mu} / \Omega_1}$ dynamic equations

$$\ddot{q}_1 = -\Omega_1^2 q_1 + 4\alpha \sqrt{1 - \bar{\mu}} \sqrt{\omega \Omega_1} Q - \frac{\alpha}{\sqrt{j}} \omega \sqrt{\Omega_1} Q^2, \tag{30}$$

$$\ddot{q}_2 = -\Omega_2^2 q_2 - 2\beta \frac{2\bar{\mu} - 1}{\sqrt{\bar{\mu}}} \sqrt{\Omega_1 \omega} Q - \frac{\beta \omega \sqrt{\Omega_2} \sqrt{1 - \bar{\mu}}}{2\sqrt{j\bar{\mu}}} Q^2, \tag{31}$$

$$\begin{aligned}
\ddot{Q} = & -\omega^2 Q + 4\alpha \sqrt{1 - \bar{\mu}} \sqrt{\omega \Omega_1} q_1 - 2\beta \frac{2\bar{\mu} - 1}{\sqrt{\bar{\mu}}} \sqrt{\omega \Omega_2} q_2 - \frac{4\alpha^2}{\Omega_1} \frac{1 - \bar{\mu}^2}{\bar{\mu}} \omega Q \\
& - \beta \sqrt{\frac{1 - \bar{\mu}}{j\bar{\mu}}} \omega \sqrt{\Omega_2} q_2 Q - \frac{\beta}{\sqrt{j}} \frac{1 - \bar{\mu}^2}{\bar{\mu}^2} \omega \sqrt{\Omega_2} q_2 Q \\
& + \frac{6\alpha^2 \omega}{\Omega_1 \sqrt{2j}} (1 - \bar{\mu})^{1/2} Q + \frac{3\beta \omega \sqrt{2\Omega_2}}{4j \sqrt{\bar{\mu}}} q_2 Q, . \tag{32}
\end{aligned}$$

Linear approach used for the normal and radiation phase far from the critical region can not be applied for the mixed critical region; Instead, nonlinear dynamic equations are to be solved. The dynamics of the level oscillator Q in (32) is influenced by the squeezing parameter $\bar{\mu}$: If j is sufficiently large, $\bar{\mu}$ is small ($\alpha^2 > \beta^2 \Omega_1 / \Omega_2$) and $\omega = 4\alpha^2 \bar{\mu} / \Omega_1 \ll \Omega_1$. It follows, that we can neglect adiabatically the intrinsic dynamics of the oscillators q_1 and q_2 and suppose it implicitly determined by the dynamics of the squeezed level polaron. (We confirmed numerically the instability of the oscillations of q_1 and q_2). Hence, we can

eliminate the oscillators q_1 and q_2 from (32) and for the squeezed level polaron Q , in the limit $j \rightarrow \infty$, i.e. $\mu \rightarrow 0$, we obtain the dynamic nonlinear equation for the classical "order parameter",

$$\ddot{Q} = \frac{16\alpha^4}{\Omega_1^2} \left(1 - \frac{\bar{\beta}^2}{\alpha^2}\right) Q + \frac{3 \cdot 2^4 \alpha^4 \bar{\beta} \sqrt{2(1 - \bar{\beta}^2/\alpha^2)}}{\Omega_1^{5/2}} Q^2 - \frac{2^6 \alpha^6 (1 - \bar{\beta}^2/\alpha^2)}{\Omega_1^3} Q^3, \quad (33)$$

or, using the transformation $Q = q + \frac{\bar{\beta}}{2\alpha} \frac{\Omega_1^{1/2}}{\sqrt{2(1 - \bar{\beta}^2/\alpha^2)}}$ the quadratic term is eliminated and one obtains the normal form

$$\ddot{q} = Aq - Bq^3 + F, \quad (34)$$

where

$$A \equiv \frac{8\alpha^2(2\alpha^2 + \bar{\beta}^2)}{\Omega_1^2}, \quad B \equiv \frac{2^6 \alpha^4 (\alpha^2 - \bar{\beta}^2)}{\Omega_1^3} > 0, \quad F \equiv \frac{4\alpha^2 \bar{\beta} \sqrt{2(1 - \frac{\bar{\beta}^2}{\alpha^2})}}{\Omega_1^{3/2}} + \frac{8\bar{\beta}^3}{\Omega_1^{3/2} \sqrt{2(1 - \frac{\bar{\beta}^2}{\alpha^2})}}. \quad (35)$$

Contrary to the previous cases, the transition described by equation (34) between the normal and radiation phase is of the first order and supports a coexistence of both phases in the sector of the normal phase $\alpha > \bar{\beta}$, or $\omega_1 > \omega_2$. We come to the conclusion that in contrast with the Dicke model the presence of the additional oscillator opens a sector of a mixed phase with partial occupation of the excitation space of all three coupled oscillators. A transition between two non-equivalent minima of the potential $V = \frac{B}{4}q^4 - \frac{A}{2}q^2 - Fq$ arises and can be considered as the oscillation-assisted tunneling (hopping). The formation of the radiation phase is driven by the force F which is compensated by the nonlinearity so that the "nuclei" (bubbles) of the radiation phase stabilize for the set of parameters (35). The exact solution to (34) is given by

$$q = a \frac{n_1 + \cos(w\tau)}{n_2 + \cos(w\tau)}, \quad (36)$$

where

$$n_1 = (2 - n_2^2)/n_2, \quad a^2 = \frac{A}{B} \frac{n_2^2}{2 + n_2^2}, \quad w^2 = 2A \frac{n_2^2 - 1}{n_2^2 + 2}, \quad a = -\frac{F}{2A} (2 + n_2^2). \quad (37)$$

The solution (36) represents nonlinear non-sinusoidal periodic oscillations. From equation (33) it is evident, that the nucleation process vanishes identically when approaching the transition point $\omega_1 = \omega_2$, where the effective polaron localization energies ω_1 and ω_2 in both

sectors are equal. Let us remind that the scenario described above can be perturbed by the fluctuations neglected by the adiabatic elimination of other two oscillators (q_1 and q_2) and by excitations due to the finite-size effects.

Let us note that, in spite of independence of Eq. (33) on j in the thermodynamic limit $j \rightarrow \infty$, the dynamic variable Q is j -dependent so that the resulting mixed phase exists only for finite j as expected.

Numerical evaluation of the order parameter J_z from the exact Hamiltonian (7) presented in Fig. 2 illustrates the existence of the intermediate phase by non-zero occupation in the neighborhood of the point $\alpha = \bar{\beta}$.

III. INTERPLAY OF QUANTUM FLUCTUATIONS AND SYMMETRY BREAKING

A qualitatively new situation occurs in the nonlinear regime at finite j , when all three oscillators couple via interplay of fluctuations due to finite j and of breaking the rotational symmetry ($|\alpha - \bar{\beta}| > 0$).

As the next step, we shall include in (11) small terms up to $O(1/j)$ to find the effect of quantum fluctuations. To elucidate the role of fluctuations and the difference between one- and two-boson cases let us apply first the method we will use in what follows to the Dicke model (2). We displace again the operators (see [7])

$$a^\dagger = c^\dagger + \sqrt{\alpha}, \quad b^\dagger = d^\dagger - \sqrt{\delta} \quad (38)$$

to exclude linear terms from Hamiltonian (2). Here, α and δ are the mean values of excitation number $\langle a^\dagger a \rangle$ and $\langle b^\dagger b \rangle$ of related bosons a and b , respectively. Putting the Ansatz (38) into (2) and eliminating linear terms, one obtains two known solutions [7]

1. $\alpha = 0, \delta = 0$, normal phase, "1"; (39)

2. $\sqrt{\alpha} = \frac{\lambda\sqrt{2j}}{\Omega} \left(1 - \left(\frac{\omega_0\Omega}{4\lambda^2}\right)^2\right)^{1/2}$, $\sqrt{\delta} = \sqrt{j} \left(1 - \frac{\omega_0\Omega}{4\lambda^2}\right)^{1/2}$, radiation phase, "2" (40)

which determine displacements of the normal phase "1" with zero number of macroscopically excited bosons, and of the radiation phase "2" at $\lambda^2 > \omega_0\Omega/4$ with both numbers $\sim j$. Then, Hamiltonian (2) for the normal phase is reproduced,

$$H_{1D} = \Omega(c^\dagger c + 1/2) + \omega_0(d^\dagger d - j) + \lambda(c^\dagger + c) \left(d^\dagger + d - \frac{d^{\dagger 2}d + d^\dagger d^2}{4j} \right). \quad (41)$$

Let us write Heisenberg equations for the phase 1,

$$i\dot{c} = \Omega c + \lambda \left(d^\dagger + d - \frac{d^{\dagger 2}d + d^\dagger d^2}{4j} \right), \quad (42)$$

$$i\dot{d} = \omega_0 d + \lambda(c^\dagger + c) - \frac{\lambda}{4j}(c^\dagger + c)(2d^\dagger d + d^2). \quad (43)$$

Within the adiabatic approximation, we can neglect the intrinsic dynamics of the level oscillator d , assuming plausibly $\Omega \ll \omega_0$. Thus, we suppose $d\langle d^\dagger - d \rangle/dt = 0$ in (43) so that the oscillator can be eliminated from this equation and put into (42). Defining then operators $\hat{q} \equiv \frac{1}{\sqrt{2\Omega}}(c^\dagger + c)$ and $\hat{\pi} \equiv i\sqrt{\frac{\Omega}{2}}(c^\dagger - c)$, the dynamic equation for the coordinate $q = \langle \hat{q} \rangle$ up to the order $1/j$ can be written:

$$\ddot{q} = -\Omega^2 \left(1 - \frac{4\lambda^2}{\omega_0\Omega} \right) q - \frac{8\lambda^4\Omega^2}{j\omega_0^3} q^3 + O(1/j^2). \quad (44)$$

If $\frac{4\lambda^2}{\omega_0\Omega} < 1$, there result oscillations with the squeezed frequency $\Omega_D = \Omega \left(1 - \frac{4\lambda^2}{\omega_0\Omega} \right)^{1/2}$ about the displaced center. The quasiclassical potential corresponding to equation (44) yields

$$V = \frac{\Omega^2}{2} \left(1 - \frac{4\lambda^2}{\omega_0\Omega} \right) q^2 + \frac{\lambda^4\Omega^2}{4j\omega_0^3} q^4 + V_0. \quad (45)$$

For each j , the potential (45) implies a second order phase transition at $\lambda_c^2 = \omega_0\Omega/4$ which has been found as the critical point of the phase transition between the normal and super-radiant phase in the Dicke model [7]. For $\lambda < \lambda_c$, the normal phase is recovered being stable while at $\lambda > \lambda_c$ the radiation phase is stable. Let us note, that the system (45) is globally stable for each finite j and the phase transition is supported by the quantum fluctuations $\sim 1/j$. The method we present here is so verified as being able to reproduce basic results known from the standard approach used before [7] and applied for the present model in previous Section.

In what follows we shall perform analogous calculations for the system with two boson modes (16). For this case, Heisenberg equations related to (16) for the phase 1 read as follows

$$\begin{aligned} i\dot{c}_1 &= \Omega_1 c_1 + \frac{2\alpha}{\sqrt{2j}} d^\dagger d, & i\dot{c}_2 &= \Omega_2 c_2 + \beta(d^\dagger + d) - \frac{\beta}{4j}(d^{\dagger 2}d + d^\dagger d^2), \\ i\dot{d} &= \frac{4\alpha^2}{\Omega_1} d + \frac{2\alpha}{\sqrt{2j}}(c_1^\dagger + c_1)d + \beta(c_2^\dagger + c_2) - \frac{\beta}{4j}(c_2^\dagger + c_2)(2d^\dagger d + d^2). \end{aligned} \quad (46)$$

For strong interaction, it is plausible to assume $\omega_1 = \frac{4\alpha^2}{\Omega_1} \gg \Omega_1, \Omega_2$ and, consequently, to apply the adiabatic approximation neglecting intrinsic dynamics of the level polaron d of high frequency ω_1 , $\dot{d} = 0$. Consequently, it can be eliminated but it determines the dynamics of the slaved modes $q_1 = (2\Omega_1)^{-1/2}\langle c_1^\dagger + c_1 \rangle$, $q_2 = (2\Omega_2)^{-1/2}\langle c_2^\dagger + c_2 \rangle$ implicitly. Hence, we use the stationary expression for $q = (8\alpha^2/\Omega_1)^{-1/2}\langle d^\dagger + d \rangle$ from (46) and put it into remaining equations for q_1 and q_2 . Up to the lowest order term in $1/\sqrt{j}$ one obtains

$$\ddot{q}_1 = -\Omega_1^2 q_1 - \frac{\beta^2 \Omega_1 \sqrt{\Omega_1} \Omega_2}{4\alpha^3 \sqrt{j}} q_2^2 \quad (47)$$

$$\ddot{q}_2 = -\Omega_2^2 \left(1 - \frac{\beta^2 \Omega_1}{\alpha^2 \Omega_2}\right) q_2 - \frac{\beta^2 \Omega_1^2 \sqrt{\Omega_1}}{\alpha^3 \sqrt{2j}} q_1 q_2. \quad (48)$$

We received the squeezed frequency of the oscillator q_2 which justifies again the use of the slaving principle for the oscillator q_1 , $\Omega_1^2 \gg \Omega_1^2(1 - \bar{\beta}^2/\alpha^2)$. Its dynamics is then implicitly ordered by the dynamics of the oscillator q_1 . Then, similarly as in the previous case, we receive

$$\ddot{q}_2 = -\frac{dV(q_2)}{dq_2}, \quad (49)$$

where

$$V(q_2) = \frac{\Omega_2^2}{2} \left(1 - \frac{\beta^2 \Omega_1}{\alpha^2 \Omega_2}\right) q_2^2 + \frac{\beta^5 \Omega_1^2 \Omega_2}{16\alpha^6 j \sqrt{2}} q_2^4 + V_0. \quad (50)$$

Equation (50) implies a continuous phase transition at $\alpha = \bar{\beta} \equiv \beta \sqrt{\Omega_1/\Omega_2}$ to the order $1/j$ for each j between the normal oscillators (48) with squeezed frequency $\bar{\omega}_2 = \Omega_2 (1 - \bar{\beta}^2/\alpha^2)^{1/2}$, ($\alpha > \bar{\beta}$), and a nonlinear sector analogous to the super-radiant phase of the Dicke model ($\bar{\beta} > \alpha$). Note that the potential for the Dicke model (45) and (50) become identical if we set $\omega_0 \equiv 4\alpha^2/\Omega$ in equation (45).

We conclude that there occurs a sequence of phase transitions for each finite j between the quasi-normal and radiation phase ($\bar{\beta} > \alpha$) because of softening (squeezing) the frequency of the oscillator $\bar{\omega}_2 =$ by the parameter $\bar{\beta}/\alpha$.

According to Eq. (26) and (27) the critical energies at both sides of the phase transitions are symmetric when changing $\alpha \leftrightarrow \beta$ and $\Omega_1 \leftrightarrow \Omega_2$. In the radiation phase, for j finite, the nonlinearity bears one-instanton solution

$$\bar{q}_{21}(\tau - \tau_0) = \pm \frac{2\alpha_1^3}{\bar{\beta}^2 \Omega_1} \sqrt{\frac{2j}{\Omega_1} \left(1 - \frac{\alpha^2}{\bar{\beta}^2}\right)} \tanh \left(\frac{\Omega_1}{\sqrt{2}} \left(1 - \frac{\alpha^2}{\bar{\beta}^2}\right)^{1/2} (\tau - \tau_0) \right). \quad (51)$$

Here, $\bar{q}_2 = q_2 \sqrt{\frac{\Omega_1}{\Omega_2}}$, $\bar{\beta} = \beta \sqrt{\frac{\Omega_1}{\Omega_2}}$. The one-instanton solution (51) is associated with the tunneling between the extrema of the potential inverted to (50) if $\bar{\beta} > \alpha$ and $\tau \rightarrow it$. Hence, at finite j 's there appears a new instanton phase as a precursor of the phase transition at the maximum softening of the frequency at $\bar{\beta} \rightarrow \alpha$ in the radiation phase. More generally, there occurs a sequence of repeated tunnelings (oscillations between two equivalent minima of a local potential) for each lattice site. The same effect occurs in the Dicke model if $4\lambda^2/(\omega_0\Omega) > 1$ (45). Moreover, in the present model, there exists the coupling between the oscillators 1 and 2 (47,48) which was neglected in the adiabatic approximation (49). In fact, within more subtle calculations there would occur tunnelings mediated by two coupled oscillators (one of them being a polaron) for each j instead of one of the adiabatic treatment.

The time of the tunneling $T = \omega_T^{-1}$ is determined by the squeezing of the frequency $\omega_T = \frac{\Omega_1}{\sqrt{2}} \left(1 - \frac{\alpha^2 \Omega_2}{\beta \Omega_1^2}\right)^{1/2}$, i.e. the tunneling ceases at the transition point. The frequency ω_T determines the curvature close to the minima of the bistable potential (50). This initial frequency enters the probability of the tunneling from the ground state of the oscillator close to the minimum during the time τ when starting at τ_0 (e.g., [38]). According to Dekker [38] the trajectory of the tunneling particle in time exhibits chaotic features if the initial frequency is squeezed. This implies that the quantum tunneling should be associated with the chaotic features inherent to finite lattice or excited spectra of the standard Dicke model (45) or our model in the present approximation. However, there is self-evident a question about the possible mechanism of chaos production due to the squeezing in this models. Going from the present considerations, instead of the strict tunneling (51), we propose a more realistic mechanism of hopping, i.e., the above mentioned tunneling between the squeezed minima assisted by the neglected (when going from (46) to (49)) nonadiabatic fluctuations of the oscillators c_1 and d coupled by the nonadiabatic nonlinear terms $\sim 1/\sqrt{j}$ and similarly of the oscillator d (43) for the Dicke model. We remark in passing that the mechanism of hopping is known, e.g., from the transport theory of disordered systems at finite temperatures [39].

IV. STATISTICAL CHARACTERISTICS OF EXCITED LEVELS AND WAVE FUNCTIONS

The distribution of the nearest neighbor level spacings (NNS) of excited quantum levels is the standard testing point for investigation of the issues in quantum chaology [36]. Recently we have reported results on NNS distribution of the molecular JT model (6) [33] which is the case $j = 1/2$, $\Omega_1 = \Omega_2$, $\alpha \neq \beta$ in the notation of the present article. It was shown that these distributions essentially deviate from the Wigner distribution typical for well developed quantum chaos. Our results show NNS distributions nonuniversal but far from the cases with higher symmetry (rotational $\alpha = \beta$ and linear $\alpha \gg \beta$, $\alpha \ll \beta$) they tend to a form close to the semi-Poisson distribution $P(S) = 4S \exp(-2S)$ already encountered in some problems, in particular in the Anderson model close to the metal-insulator transition [40]. The peculiarity of the Jahn-Teller system with equal frequencies was that the Wigner-Dyson level spacing distribution has never been reached, and the said semi-Poisson form of the statistics appeared to be the most “chaotic” one.

In this section we present statistical characteristics (NNS distributions, entropy of level occupation, and spectral density of states) of the spectra for $\Omega_1 \neq \Omega_2$, $j \geq 1/2$. We solved numerically the eigenvalue problem for the quantum Hamiltonian (7). The Hamiltonian was diagonalized with the basis of the boson Fock states for bosons 1 and 2. When taken N_1 and N_2 Fock states for each of $2j + 1$ electron levels, there is produced an inevitable truncation error, so that the results were checked against the convergence (with changing the numbers N_1, N_2). Only about ~ 1100 lower states were used for calculating the statistics out of typically $\sim (8 \div 10) \times 10^3$. The obtained raw energy spectrum had to be treated by an unfolding procedure in order to ensure the homogeneity of the spectrum (constant local density of levels). Thereafter the statistical data were gathered in a standard fashion from small intervals in the space of parameters (α, β) . The calculations were performed essentially along the same lines as our previous calculations for the Jahn-Teller problem with $j = 1/2$ [33, 35] where additional details were given as to the convergence check, unfolding procedure and gathering statistics.

The results for the level spacing distributions for different phonon frequencies $\Omega_1 \neq \Omega_2$ and $j > 1/2$ show rather vast variety ranging from Wigner to Poisson distributions as limiting cases but recovering also the semi-Poisson distribution in a rather wide range of

model parameters. With increasing j , general tendency consists in increasing the diapason of parameters where the NNS shows deviations from the Poisson distribution towards chaoticity up to the maximum degree of chaoticity given by the Wigner distribution. So, for the case $j = 1/2$ and equal frequencies the maximal degree of chaoticity being expressed by the semi-Poisson distribution in accord with our previous results. For moderate j ($j = 7/2$ and $\Omega_1 \neq \Omega_2$ exemplified in 3 there appears a well-marked domain of maximal chaoticity (Wigner distribution). For example, for $\Omega_2/\Omega_1 = 2$ the domain of Wigner distribution stretches for the values of parameters $1 \lesssim \alpha, \beta \lesssim 3$.

We can conclude that the presented results essentially deviate from the Wigner statistics of levels imposed by the one-boson Dicke model [7]. For comparison, we performed the same calculations of NNS distributions for the standard one-boson Dicke model (Fig. 4). The distributions follow closely the Wigner form of the $P(S)$ curve, but a good agreement is achieved only for high values of j . For the resonance case $\Omega_1 = \Omega_2$ the quantum chaotic statistics (Wigner surmise [36]) changes towards a non-universal with respect to α, β but tending to the semi-Poisson intermediate statistics achieved asymptotically far from the cases of the special symmetry (rotation, linear). In contrast to one-boson models, this universality is observed even for small number of electron levels and seems not to change with raising j . Therefore the impact of the second boson mode is that it essentially changes the quantum statistics. For the non-resonance case $\Omega_1 \neq \Omega_2$ we observe a considerable suppression of chaos manifesting in the reduction of the “pure” domain of Wigner chaos in the space of the parameters α, β .

To visualize the wave functions of the excited levels of the system we considered the spreading of the wave functions over the electron levels and integrated out two boson degrees of freedom. Thus we found numerically the probability $P_i^{(n)}$ of the wave function $\phi_i^{(n)}$ to occupy a given electronic level i of the system. The full wavefunction depending on both vibron and electron level variables is calculated by the same scheme of the diagonalization of the quantum Hamiltonian in the representation of Fock states as described above. If $\beta = 0$, Hamiltonian equation is split onto $N(= 2j + 1)$ independent equations labeled by $i = 1, \dots, (2j + 1)$, so that the wavefunction for each given state n is localized on some electron level i . If $\beta \neq 0$, Hamiltonian matrix is no more diagonal (since J_x is nondiagonal), so that its components get interacting. The resulting eigenfunction is in general $(2j + 1)$ -fold function occupying each electronic level (see Chapter 1 as for the discussion about

normal and super-radiant phase in the thermodynamic limit). Let $\chi_i^{(n)}(Q_1, Q_2)$ be the i -th component of the $(2j+1)$ -dimensional vector of the eigensolution of the Hamiltonian matrix equation for n -th energy level in the "coordinate" representation ($\hat{Q}_l \propto b_l^\dagger + b_l$, $l=1,2$). Then the occupation probabilities of the i -th electronic level are $P_i^{(n)} = \iint |\chi_i^{(n)}|^2 dQ_1 dQ_2$. In this representation we exemplify the wave functions in Fig. 5 for the levels $n = 1, 4$ and the parameters around the point of QPT $\alpha = 2$, $\beta = 1.95, 2.05$ and $\Omega_1 = \Omega_2$. The abrupt change in the shape of wavefunctions when going from normal to super-radiant phase is easily perceivable not only for the ground state, but for lowest excited states as well (in this example for $n=4$). However, for higher excited states the wavefunctions generally spread over the whole available electron space, irrespective to the relation between α and β . The last relation is also reflected in the statistical properties of levels: they are invariant with respect to the exchange $\alpha \leftrightarrow \beta$, $\Omega_1 \leftrightarrow \Omega_2$, likewise it was already shown for the generalized JT model [33]. In order to characterize quantitatively the behavior of the wavefunctions of excited states we introduce the entropy of level occupation

$$S_n = - \sum_{i=1}^N P_i^{(n)} \log P_i^{(n)}, \quad (52)$$

where $\sum_{i=1}^N P_i^{(n)} = 1$. In Fig. 6 for $\Omega_1 = \Omega_2$ we plot the said entropies for first 1000 quantum levels of a system with four electron levels ($j = 3/2$). One can see from these figures that in the most excited states the electronic levels are equally populated (with probabilities $1/(2j+1)$, e.g., last Figure in Fig. (5)), thus the said entropies tend to their limiting value $\log(2j+1)$. For four levels the entropy yields the value $S_4 = 2 \log 2 = 1.38$ which is confirmed by Fig. 6 for $\alpha \neq \beta$. However, among these extended states there emerge "localized" levels of lower values of the entropy which are characterized by a relative localization of wavefunction on smaller number of electron levels. Such levels form marked branches seen in Fig. 6, which remind of the branches of "exotic" states in the generalized Jahn-Teller model [34]. Most of the states show an intermediate degree of localization between both of the limits. These intermediate electronic states correspond to the mixed intermediate domain of the normal and radiation phase in the respective boson space.

Another way to visualize the complex structure of the excited states and corresponding wave functions is the representation of the spectral density given by the imaginary part of the projected resolvent [42]. It shows the characteristic frequencies of the final state of the

evolution of a system starting from the projected Hilbert space and returning to it. The spectral density of states $F(E)$ can be defined with respect to some initial state $|\Psi_0\rangle$ (the ground state, see below) and is connected with the return probability to this state in the course of the system evolution through the exact states Φ_n , eigenfunctions of the energies E_n of the system at small $\varepsilon \sim 0$:

$$F(E) \equiv \text{Im}\langle\Psi_0|(E - \hat{H} - i\varepsilon)^{-1}|\Psi_0\rangle = \varepsilon \sum_n \frac{|\langle\Phi_n|\Psi_0\rangle|^2}{(E - E_n)^2 + \varepsilon^2}, \quad (53)$$

where $|\Phi_n\rangle$ and E_n are the eigenfunctions and corresponding eigenvalues of the Hamiltonian \hat{H} . The small parameter ε fixes the rules of handling the poles of the Green function in the complex space. In Fig. (7) we show the examples of the spectral density for the values of parameters α, β below and above the critical line. As the initial state $|\Psi_0\rangle$ we took the ground state with $\alpha = \beta = 0$, that is the product of the electronic Dicke state $|j, -j\rangle_{el}$ and the phonon state $|0, 0\rangle_{ph}$ with zero number of both bosons 1 and 2. Thus the spectral density in Fig. (7) characterizes the evolution of the system with the interactions α, β switched on in the initial time. The peaks at each E_n measure the overlap between the initial state Ψ_0 and the eigenstate Φ_n for $\varepsilon \sim 0$.

V. CONCLUSION

The numerical analysis of the generalized (two boson modes with different frequencies) Dicke model or the equivalent generalized lattice JT model with fully broken local rotation symmetry (different coupling constants $\alpha \neq \beta$ and different frequencies $\Omega_1 \neq \Omega_2$) brings following new results:

(i) The critical point of the second order phase transition, (1), is modified to $\alpha = \beta\sqrt{\frac{\Omega_1}{\Omega_2}}$ when compared with the critical point of the one-boson Dicke model $\alpha = \beta$. The renormalization of the couplings by the frequencies is due a reformulation of the critical point in terms of frequencies of the dressed oscillators as $\omega_1 = \omega_2$, $\omega_1 = \frac{4\alpha^2}{\Omega_1}$, $\omega_2 = \frac{4\beta^2}{\Omega_2}$.

(ii) The electron level order parameter $\langle J_z \rangle / j$ (2) shows the finite size effect for finite j close to the phase transition point which smoothes the phase transition to a rather broad at small j "mixed" region. The effect is slightly nonsymmetric around the critical point supporting the order parameter in the normal phase.

(iii) The level spacing probability distribution (3) of the model under consideration bears a drastic change from the Wigner-Dyson $P(S) \sim S \exp(-S^2)$ distribution of the one-boson Dicke model (4) by a non-universal transition up to close to the Poisson distribution $P(S) \sim \exp(-S)$. For equal frequencies, $\Omega_1 = \Omega_2$ and different coupling constants, however, the distribution ranges non-universally from a close to the semi-Poisson $P(S) = 4S \exp(-2S)$ to the Poisson distribution. Evidently, the change to the range between the Wigner-Dyson and the semi-Poisson distribution is due to the difference in the frequencies.

(iii) In the electron space, the phase transition reveals in a drastic change of the wave functions from those spread over small number of levels (sites) in the "normal" phase to the macroscopic distribution of the excitation over all the levels (lattice) in the radiation phase, (5). This behavior shows up a non-universality with regard to the interaction parameters and inhomogeneity throughout the spectral levels.

(iv) Entropies of occupation of the electronic levels (5) illustrate the measure of localization of the states throughout the spectra (or the lattice). There is evident the asymptotic line of the delocalized states at $S = 1.38$ and the localized states with various extent of localization. Close to the line from below there is evident a relatively high density of weakly correlated states. The lowest levels show up branches of the localized states. Let us remind that the exceptional case of $\alpha = \beta$ belongs to a higher class of symmetry out of the concept of the present paper.

(v) A measure of the localization of the spectral states as a function of energy is the spectral density of states (7). It measures the evolution of the states from the pure Dicke states ($\alpha = \beta$) in $t = 0$ to the exact numerical states of the system at interactions switched on at $t > 0$. During the evolution of the system to the final state the system overlaps with the initial state at the poles of respective propagator $F(E)$ (53). The peaks of the function $F(E)$ measure the overlap between the initial Dicke states Ψ_0 and the exact eigenstates $\Phi_n(E)$ for $\varepsilon \sim 0$.

Beside the exact numerical analysis, use of the Holstein-Primakoff Ansatz made us possible to treat analytically, though approximately, the present model. The analytical treatment brings a useful insight into the mechanisms behind of the properties illustrated by the numerical results. We have shown that an additional boson mode coupled with the electron level spacing dresses the normal-phase oscillator to a self-trapped one similarly as it was dressed the oscillator in the radiation phase. This mode-dressing modified by squeezing cooperates

with nonlinear terms at finite j : It modifies both the normal and the radiation phase close to the transition point $\alpha = \beta \sqrt{\frac{\Omega_1}{\Omega_2}}$. The intermediate region of the "nucleation" occurs as a consequence of the competition of the self-localization due to the polaron dressing modified by squeezing of the level boson mode and of the boson-assisted tunneling. Both quasi-normal and radiation phases coexist within the sector of the quasi-normal phase $\alpha > \bar{\beta}$. We have shown that the formation of the radiation phase is driven by the boson-assisted tunneling (hopping) and is compensated by the nonlinearity due to the selftrapping so that the "nuclei" of the radiation phase get stabilized. So, in contrast with the one-boson Dicke model, for finite j the additional oscillator opens a sector of a "quantum mixed phase" with partial occupation of the excitation space of all three coupled oscillators.

We have shown that in the radiation phase there occurs a sequence of repeated tunnelings (oscillations between two equivalent minima of a local potential) for each lattice site. The radiation phase can be then represented as an almost ideal instanton–anti-instanton gas phase (instanton lattice). However, there exists a weak coupling with two oscillations assisting the tunneling because of non-adiabatic fluctuations due to the finiteness of the lattice. They are necessarily involved by the model and moderate the polaron dressing of the level mode (29). As a result, they perturb the ideal periodicity of the instanton lattice. In a variable extent the quantum fluctuations due to the level correlations persist within the whole radiation phase and represent the dephasing mechanism of thorough coherence of the phase. We have shown that the sequence of local "second-order phase transitions" and so the instanton–anti-instanton gas phase exists in the standard one-boson Dicke model as well, in contrast to the mixed phase which does not exist in this model.

Numerical calculations show reflection of the described three phases in the statistical properties. We have demonstrated a drastic qualitative change of the level spacing probability distributions from the universal Wigner of the one-boson Dicke model to the non-universal transition from the Wigner distribution of the localized states of the quasi-normal phase through the critical semi-Poisson distribution of the mixed domain to a close-to-Poisson distribution for the almost ordered radiation phase. This change is attributed to the weakening of the Wigner chaos caused by the tunneling mechanism mediated by the additional mode. The fluctuation effects in the "radiation" phase are respectively weakly j -dependent for small j .

For finite lattice systems, where the localization-delocalization phase transitions occur,

we suggest possibility to apply the present results to interpret finite-size fluctuation effects. We propose the applications of the presented results for finite systems where fluctuations destroy quantum coherence and a second order phase transition is modified by the tunneling mediated by the fluctuations. The destroying the coherence of the radiation phase by the boson selftrapping is a source of the dephasing mechanism in the radiation phase. The spectral phenomena as is the inhomogeneous broadening of the zero-phonon spectral lines and the broadening of spectra are due to the selftrapping in the quasi-normal phase. This interpretation can be applied, e.g., as a mechanism responsible for the inhomogeneous broadening of the zero-phonon lines of the Dicke superfluorescence in KCl [25].

The finite-size fluctuations enable the formation of a critical phase of mixed localized and delocalized phases. An example of such a system with analogous picture of quantum phase transition provides the ultracold Bose gas in an optical lattice where the phase coherence of Bose atoms is destroyed by the suppression of the tunneling due to the localization by the strong lattice potential [42], [43]. From the competition of the tunneling and the localization due to the lattice there results the phase transition between the highly coherent superfluid phase of Bose atoms and the localized Mott insulating phase of the atoms on the lattice [41]. If some fluctuations, e.g., due to lattice vibrations, mediated the tunneling within the insulating phase, as well as perturbed the coherence of the coherent superfluid phase, the system of Bose atoms in the optical lattice would exhibit analogous properties as those of the two-boson Dicke model.

We propose also the additional mode as a mean to reduce chaos in related spectral properties of optical devices based on the Dicke model.

Acknowledgement The financial support by the project No. 2/0095/09 of the Grant Agency VEGA of the Slovak Academy of Sciences is highly acknowledged.

-
- [1] P. Graham, and M. Höhnerbach, *Z. Phys. B* **57**, 233 (1984).
 - [2] P. Graham, and M. Höhnerbach, *Phys. Lett. A* **101A**, 61 (1984).
 - [3] C.H. Lewenkopf, M.C. Nemes, V. Marvulle, M.P. Pato, and W.F. Wreszinski, *Phys. Lett. A* **155** 113 (1991).
 - [4] M. Cibils, Y. Cuche, and G. Müller, *Z. Phys. B* **97**, 565 (1995).

- [5] R. H. Dicke, Phys. Rev. **93**, 99 (1954).
- [6] C. Emary, T. Brandes, Phys. Rev. Lett. **90**, 044101 (2003).
- [7] C. Emary, T. Brandes, Phys. Rev. E**67**, 066203 (2003).
- [8] K.-D. Harms, and F. Haake, Z. Phys. B **79**, 159 (1990); S. Gnutzmann, F. Haake, and M. Kus, J. Phys. A **33**, 143 (2000).
- [9] D. Tolkunov, and D. Solenov, Phys. Rev. B **75**, 024402 (2007).
- [10] P. Pfeifer, Phys. Rev. A **26**, 701 (1982).
- [11] J. Larson, Phys. Rev. A **78**, 033833 (2008).
- [12] N. Skribanowitz, I. P. Herman, J.C. MacGillivray, and M. S. Feld, Phys. Rev. Lett., **30**, 309 (1973).
- [13] M. Gross, and S. Haroche, Physics Reports **93**, 301 (1982).
- [14] A. V. Andreev, V. I. Emel'yanov, and Yu. A. Il'inskii', Sov. Phys. Usp. **23**, 493 (1980).
- [15] R. Florian, L.O. Schwan, and D. Schmid, Phys. Rev. A **29**, 2709 (1984).
- [16] R. G. DeVoe, and R. G. Brewer, Phys.Rev.Lett **76** 2049 (1996).
- [17] T. Brandes, and B. Kramer, Physica B **284** 1774 (2000).
- [18] T. Brandes, Phys. Repts, **408**, 315-474 (2005).
- [19] T.C. Jarett, A. Olaya-Castro, and N. F. Johnson, J. Phys. Conference Series, **84**, 012009 (2007).
- [20] M. O. Scully, Y. Rostovtsev, A. Svidzinsky, and J-T. Chang, J. Mod.Optics **55**, 3219 (2008).
- [21] I.L. Kuusmann, P.K. Liblik, and Ch. B. Lushchik, JETP Lett., **21**, 72 (1975).
- [22] H. J. Kmieciak, M. Schreiber, T. Kloiber, M. Kruse, and G. Zimmerer, J. Lumin. **38**, 93 (1987).
- [23] T. Kishigami-Tsujibayashi, and K. Toyoda, T. Hayashi, Phys. Rev. B **45**, 13 737 (1992).
- [24] Xiaoya Ding, and John C. Wright, Chem. Phys. Lett. **269**, 341 (1997).
- [25] M. S. Malcuit, J. J. Maki, D. J. Simkin, and R. W. Boyd, Phys. Rev. Lett. **59**, 1189 (1987).
- [26] A. Köngeter and M. Wagner, J. Chem. Phys. **92**, 4003 (1990); A. Köngeter and M. Wagner, J. Lumin. **45**, 235 (1990).
- [27] H. Eiermann and M. Wagner, J. Chem. Phys. **96**, 4509 1992.
- [28] J. C. Slonczewski, Phys. Rev. **131**, 1596 (1963).
- [29] S. E. Canton, A. J. Yench, E. Kuk, J. D. Bozek, M. C. A. Lopes, G. Snell, and N. Berrah, Phys. Rev. Lett., **89**, 045502 (2002).
- [30] E. Majerníková, J. Riedel, and S. Shpyrko, Phys. Rev. B **65**, 174305 (2002).

- [31] H.C. Longuet-Higgins, U. Öpik, and M. H. L. Pryce, Proc. Roy. Soc. London, Ser. **A244**, 1 (1958).
- [32] E. Majerníková and S. Shpyrko J. Phys.: Cond. Matter **15**, 2137 (2003).
- [33] E. Majerníková and S. Shpyrko, Phys. Rev. E **73**, 057202 (2006).
- [34] E. Majerníková and S. Shpyrko Phys. Rev. E **73**, 066215 (2006).
- [35] E. Majerníková and S. Shpyrko, J. Phys. A: Math. Theor. **41**, 155102 (2008).
- [36] F. J. Dyson and M. L. Mehta, J. Math. Phys. **4**, 701 (1963).
- [37] T. Holstein, H. Primakoff, Phys. Rev. **58**, 1098 (1949).
- [38] H. Dekker, J. Phys. A: Math. Gen. **19**, L1137 (1986).
- [39] H. Overhof, J. Non-Cryst. Sol., **227-230**, 15 (1998).
- [40] B. I. Shklovskii, B. Shapiro, B. R. Sears, P. Lambrianides and H. B. Shore, Phys. Rev. B **47**, 11487 (1993).
- [41] M. P. A. Fisher, P. B. Weichman, G. Grinstein and D. S. Fisher, Phys. Rev. B **40**, 546 (1989).
- [42] K.Ziegler, Phys.Rev.B **72**, 075120 (2005).
- [43] R. Roth and K. Barnett, J. Phys. B: At. Mol. Opt. Phys. **37**, 3893 (2004).

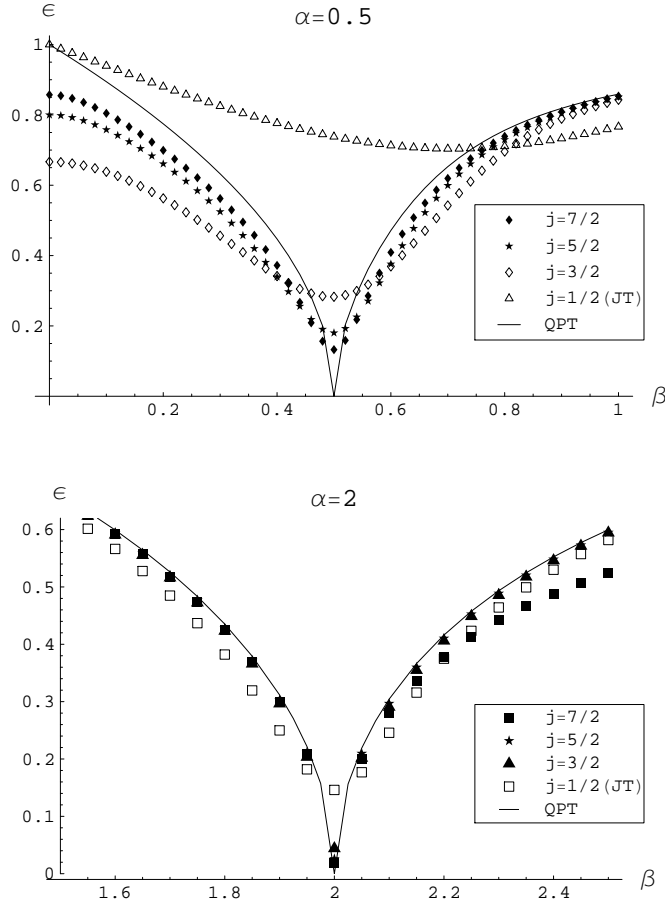


FIG. 1: Phase transition between the normal and radiation phase in the generalized Dicke and J-T lattice model for $\alpha = 0.5, 2$ and resonance case $\Omega_1 = \Omega_2 = 1$. The symbols show the numerical results for the excitation energy of the first excited state for different j , the solid line in each figure is the analytical result for QPT (18), (24) valid for $j \rightarrow \infty$. The cusp-like behavior at the critical point $\omega_1 \equiv 4\alpha^2/\Omega_1 = 4\beta^2/\Omega_2^2 \equiv \omega_2$ appears already for relatively small number of sites, e.g., for $j = 7/2$. For small j , the fluctuations smooth the cusp especially at weak couplings. The non-symmetry about the critical point by the reduction of the energy in the radiation phase for $\alpha = 0.5$ is due to the effect of quantum fluctuations (squeezing) and vanishes with increasing j and α . For the case of different $\Omega_1 \neq \Omega_2$ the picture is qualitatively the same, there occurs a shift of the transition point inwards the phase with higher Ω_i .

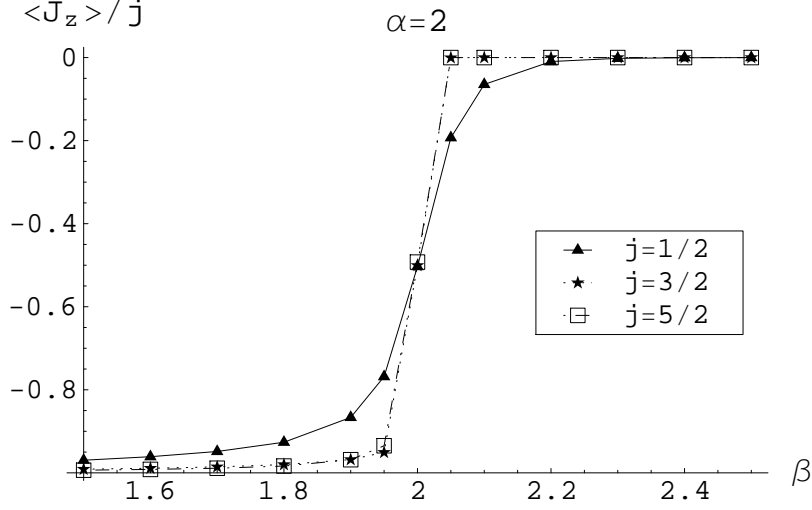


FIG. 2: Order parameter $\langle J_z \rangle / j$ for $j = 1/2, 3/2, 5/2$ and $\Omega_1 = \Omega_2$. The finite-size effect (j finite) of the mixed phase about the transition vanishes for $j \rightarrow \infty$.

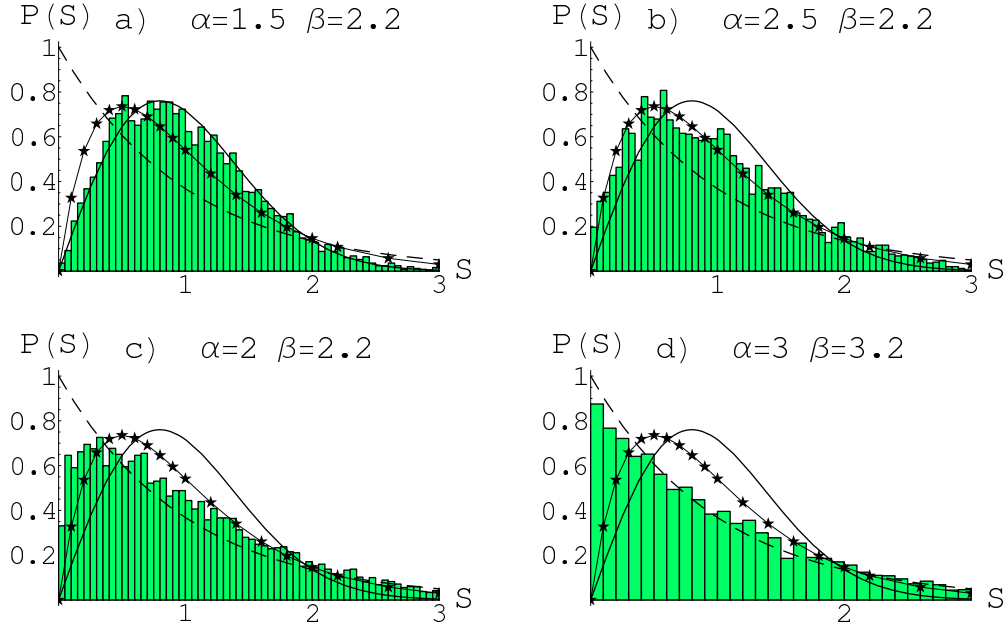


FIG. 3: Level spacing distributions for $j = 7/2$ and different (α, β) (parameters are scaled to $\Omega_1 = 1$). Upper row ((a,b)): $\Omega_2 = 2\Omega_1$; bottom row ((c,d)): $\Omega_2 = 0.5\Omega_1$. The curves show Wigner (solid), Poisson (dashed) and semiPoisson (stars) distributions. NNS distributions in b), c) are close to the semi-Poisson distribution $P(S) = 4S \exp(-2S)$ [33]; histograms in a) and d) are almost perfect Wigner ($P(S) \sim S \exp(-S^2)$) and Poisson $P(S) = \exp(-S)$ distributions.

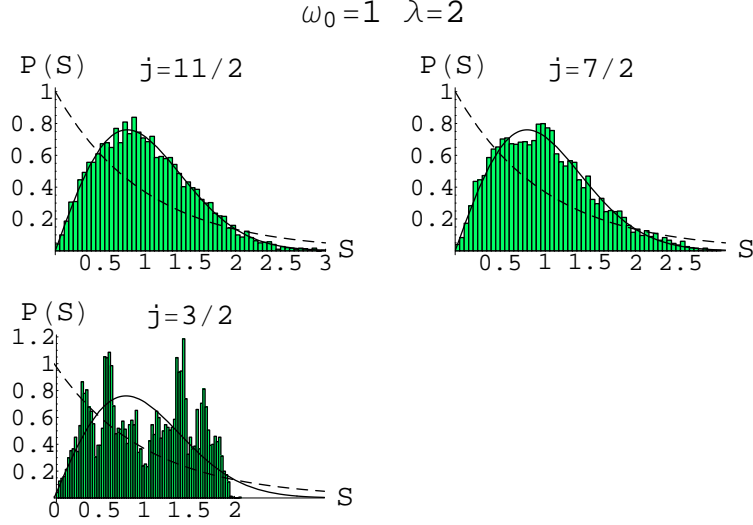


FIG. 4: Level spacing distributions for one-boson Dicke model (2) (boson frequency Ω scaled to 1). At large $j = 7/2, 11/2$ almost pure Wigner chaos $P(S) \sim S \exp(-S^2)$ is revealed. The smaller j , the stronger are level fluctuations growing with decreasing λ .

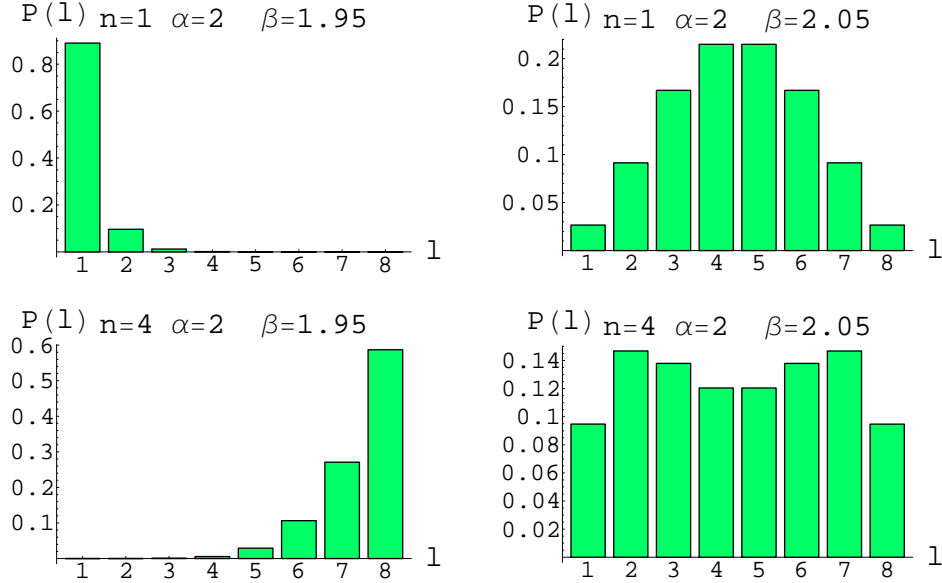


FIG. 5: The occupations $P(l)$ of the electronic levels $l = 1, \dots, 2j + 1$ (see Sect. IV.) close the the critical point $\alpha = \beta$ ($\Omega_1 = \Omega_2 = 1$; $j = 7/2$) of the phase transition between the quasi-normal and radiation phase for the ground $n = 1$ and fourth $n = 4$ excited state. For $\Omega_1 \neq \Omega_2$ the occupations remain qualitatively the same.

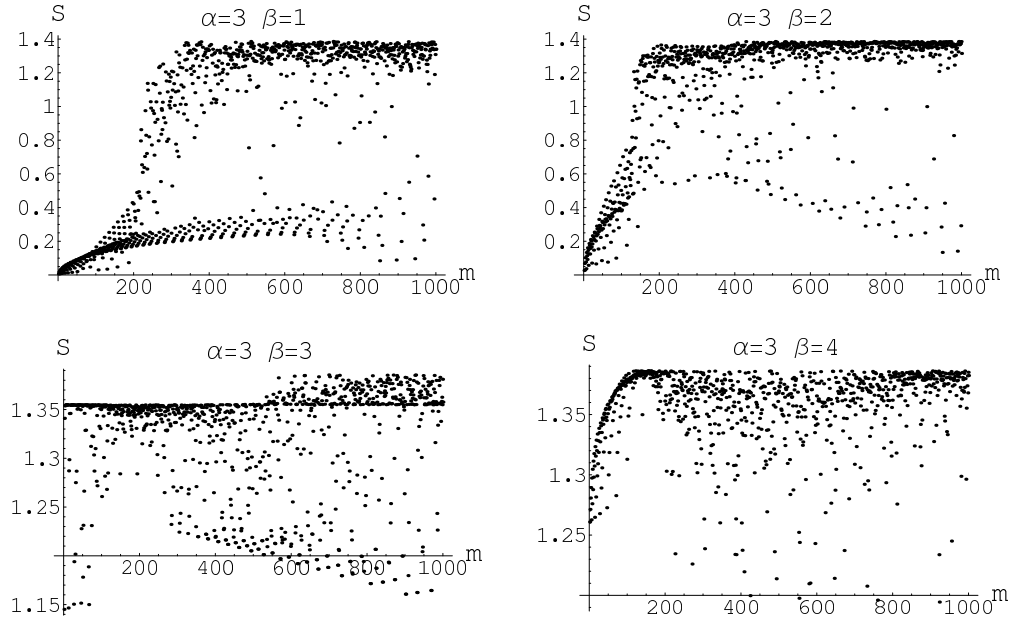


FIG. 6: Entropies of occupation of electronic levels (52) as function of the number of excited state m for $j = 3/2$ (4 levels). The states with entropy lower than the limiting value $\log(2j + 1)$ have larger measure of localization.

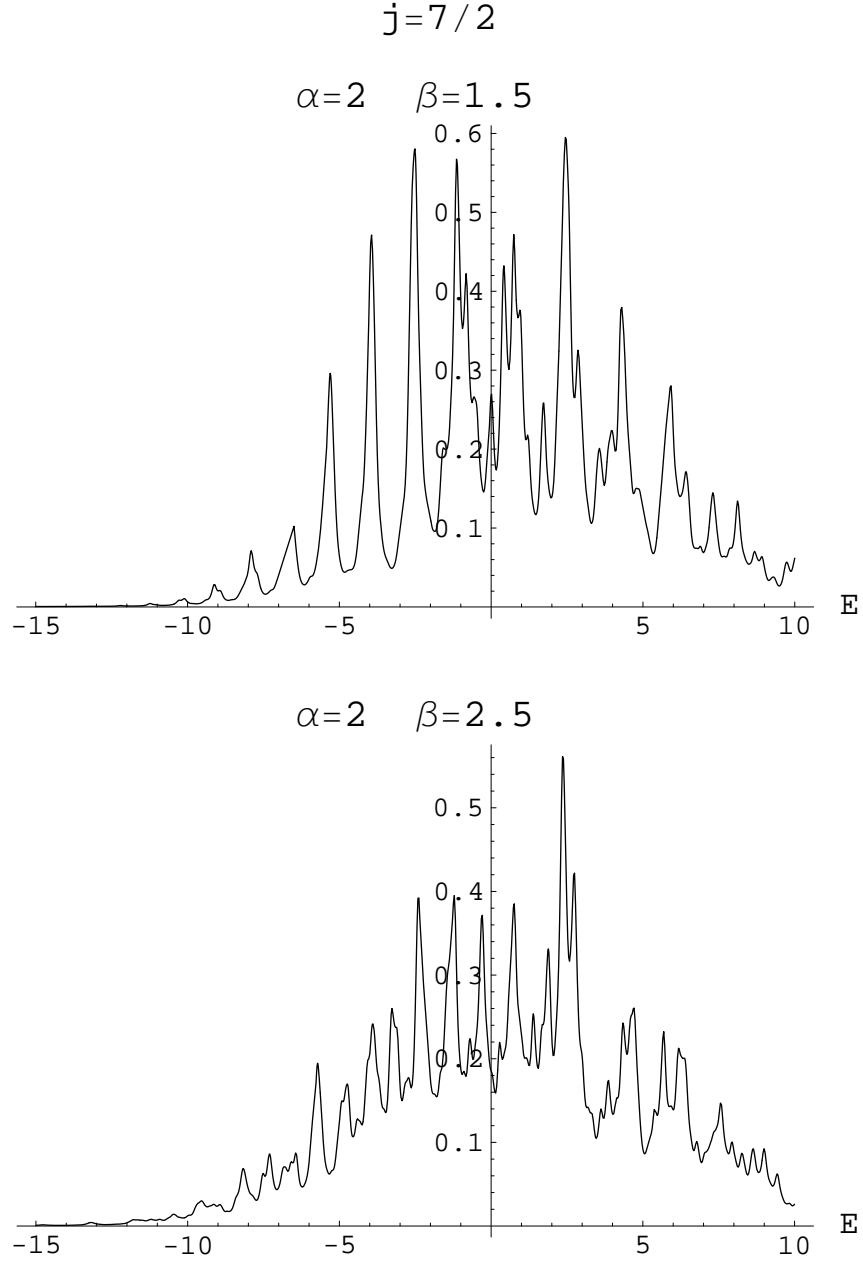


FIG. 7: Examples of the spectral density of states $F(E)$ (53) for $\alpha = 2$ and $\beta = 1.5, 2.5$ (We plot the resonant case $\Omega_1 = \Omega_2 = 1$; $j = 7/2$; the non-resonant cases do not change the picture qualitatively. The same applies for previous two Figs.)